The Journal of Experimental Biology 211, 587-598
Published by The Company of Biologists 2008
doi:10.1242/jeb.012096

Speed-dependent intrinsic caudal fin muscle recruitment during steady swimming in bluegill sunfish, *Lepomis macrochirus*

Brooke E. Flammang* and George V. Lauder
Museum of Comparative Zoology, Harvard University, 26 Oxford Street, Cambridge, MA 02138, USA
*Author for correspondence (e-mail: bflammang@oeb.harvard.edu)

Accepted 3 December 2007

SUMMARY

There are approximately 50 muscles that control tail fin shape in most teleost fishes, and although myotomal muscle function has been extensively studied, little work has been done on the intrinsic musculature that controls and shapes the tail. In this study we measured electrical activity in intrinsic tail musculature to determine if these muscles are active during steady rectilinear locomotion, and to compare intrinsic muscle recruitment patterns to previous data on myotomal muscle fibers. Five bluegill sunfish (*Lepomis macrochirus*) were anaesthetized and electrode wires surgically placed into a total of 24 intrinsic caudal muscles, up to 13 at a time, and activity was correlated with synchronous recordings from myotomal fibers in the caudal peduncle. After recovery, fish swam steadily at speeds of 0.5, 1.2 and 2.0 $L\ s^{-1}$, while filmed from lateral, posterior and ventral views simultaneously at 250 frames s^{-1}. Comparison among speeds confirmed that muscle recruitment varies significantly with speed. At 0.5 $L\ s^{-1}$, the caudal fin was generally not used for propulsion, and swimming was accomplished primarily through body undulations. Intrinsic caudal muscle activity at this speed was intermittent and variable. At 1.2 and 2.0 $L\ s^{-1}$, the supracarinalis and infracarinalis muscles acted on the dorsal- and ventral-most fin rays, respectively, to expand the surface area of the caudal fin. The interradialis muscles adducted individual fin rays, dorsally to ventrally, following activation of the hypochordal longitudinalis. Contralateral muscle activity of interradialis muscles occurred as the caudal fin crossed the mean direction of travel and fin height was greatest, whereas ipsilateral activity of carinalis muscles occurred near points of maximum excursion of the fin, at speeds of 1.2 and 2.0 $L\ s^{-1}$, after fin height was lowest. Burst intensity increased with swimming speed, suggesting stiffening of the tail fin against imposed hydrodynamic loads. Activity patterns of intrinsic caudal muscles suggest that these most posterior muscles in fishes, located within the tail, are among the very first recruited as swimming speed increases, and that slow undulatory swimming is powered by muscle fibers located posteriorly in the caudal peduncle and tail.

Key words: fish, swimming, locomotion, kinematics, electromyography, muscle, caudal fin.

INTRODUCTION

The caudal fin of fishes, with its large surface area, is of major importance for propulsion, and general patterns of fin motion have often been studied to quantify the frequency and amplitude of tail beats during locomotion (Bainbridge, 1963; Grove and Newell, 1936; Lauder, 1989; Nursall, 1958; Videler, 1975; Webb and Smith, 1980). A few three-dimensional kinematic analyses have provided additional information on complex patterns of motion of the caudal fin (Ferry and Lauder, 1996; Gibb et al., 1999; Tytell, 2006), but there is virtually no information on how movements of the caudal fin are controlled and on how caudal fin muscles are recruited during steady swimming in fishes.

Anatomical studies of caudal fin structure (Lauder, 1982; Lauder, 1989; Liem, 1970; Nag, 1967; Videler, 1975; Winterbottom, 1974) have shown that approximately 50 discrete muscles are present within the caudal fin, and that these muscles could potentially control tail fin shape during swimming and generate propulsive waves on the caudal fin itself independently of the myotomal muscle fibers that generate body bending anterior to the tail. Intrinsic caudal musculature is derived from the overlying axial body muscles, but is modified into smaller muscle groups that do not resemble the broad 'w-shaped' myomeres of the axial body musculature in either form or function. Instead, intrinsic caudal muscles are compartmentalized into small specific muscle groups that insert onto and are proposed to control specific fin rays or groups of fin rays (Gemballa, 2004; Lauder, 1982; Nag, 1972; Winterbottom, 1974). Muscular activity patterns that could control the shape and orientation of the caudal fin in teleost fishes have yet to be described [although some preliminary data have been presented by Lauder (Lauder, 1989) and Videler (Videler, 1975)], and there are effectively no data on recruitment patterns for intrinsic tail musculature in fishes.

To this end, the overall goal of this work was to establish a baseline understanding of intrinsic caudal muscle activity patterns in fishes by examining muscle activity in relation to caudal fin kinematics during steady swimming at different speeds. Determining activity patterns of intrinsic caudal muscles will allow for better understanding and linkage of the anatomical structure of the caudal fin in fishes (Gemballa, 2004; Lauder, 1982; Lauder, 1989; Lauder and Drucker, 2002; Liem, 1970; Nag, 1967; Videler, 1975; Winterbottom, 1974) with kinematic patterns and previous studies of caudal fin wake hydrodynamics (Bainbridge, 1963; Breder, 1926; Gibb et al., 1999; Nauen and Lauder, 2002; Tytell, 2006; Videler, 1975).

This study addresses four specific questions. First, are intrinsic caudal fin muscles active during steady swimming behaviors in fishes, or are these muscles only used to modulate tail shape during maneuvers and hovering behavior where complex tail motions are most evident? We hypothesize that intrinsic caudal fin muscles will be active during steady swimming, albeit at lower intensities than

muscle activity during complex tail motions. Second, if intrinsic tail muscles are active during steady rectilinear locomotion, when are they first recruited as swimming speed increases? We expect that intrinsic caudal muscle activity will first be prevalent near swimming speeds of one body length per second, when bluegill sunfish begin to utilize body–caudal swimming instead of pectoral fin locomotion. Third, are there differential activity patterns evident among the many intrinsic tail muscles, or do they tend to be active as a group? We predict that differential muscle activity will be observed, acting to control modulation of the tail fin during swimming. Fourth, how does the recruitment pattern of intrinsic caudal fin musculature compare to patterns previously described for myotomal red and white fibers? We anticipate that the patterns observed in previous studies on red and white myotomal muscle in bluegill sunfish will be conserved in the intrinsic caudal musculature (Jayne and Lauder, 1994).

MATERIALS AND METHODS

Fish

Bluegill sunfish, *Lepomis macrochirus* Rafinesque, were collected using seine nets in ponds near Concord, MA and maintained in the lab at room temperature (~20°C) in individual 40 l aquariums, where they were fed three times a week. Fish were placed in the working section of a recirculating flow tank 2 days before the experiments and were not fed during this time. After 8 h in the flow tank on the first day, the flow was turned on to approximately 1 body length per second ($L\ s^{-1}$) for 10–15 min to see if fish would be able to orient into the flow and swim without difficulty. All fish were induced to swim within the center region of the flow tank, away from the walls, as in our previous studies of fish locomotion (Drucker and Lauder, 2005; Jayne and Lauder, 1995b; Liao and Lauder, 2000; Standen and Lauder, 2005; Tytell, 2006). On the second day the fish were allowed to rest with the flow turned off. Experiments were conducted on the third day. A total of seven fish of similar size were used in this study (17.5±0.80 cm total length, TL, mean ± s.e.m.), five for kinematic and electromyography experiments, one for electrical stimulation of caudal fin muscles, and one for computer microtomography (μCT) scanning.

Kinematic protocol

Experimental data were gathered while each of five sunfish swam in a 600 l recirculating tank, which had a 26 cm×26 cm×80 cm study area, as in previous research (Standen and Lauder, 2005; Tytell, 2006). Three high-speed digital video cameras (Photron USA, Inc., San Diego, CA, USA) were used to record the lateral, posterior and ventral views of the fish. Each fish was filmed at 250 frames s^{-1} (with 1024×1024 pixel resolution) while swimming steadily at speeds of 0.5, 1.2 and 2.0 $L\ s^{-1}$.

High-speed video was calibrated using direct linear transformation of a custom 20-point calibration frame in three dimensions and digitized using a program written for MATLAB 6.5.1 (MathWorks, Inc., Natick, MA, USA) by Ty Hedrick (Hatze, 1988; Hedrick et al., 2002; Hsieh, 2003; Standen and Lauder, 2005). A total of 7 points were digitized from the video in the caudal region of each fish: (1) the posterior end of the second fin ray, (2) the posterior end of the sixth fin ray, (3) the posterior end of the ninth fin ray in the fork of the caudal fin, (4) the posterior end of the twelfth fin ray, (5) the posterior end of the fifteenth fin ray, (6) at the insertion of the anal fin on the anterior ventral edge of the caudal peduncle, and (7) at the posterior ventral edge of the caudal peduncle at the base of the first raylet. A total of 33 tail beat sequences from three fish with good electrode placement and consistently steady swimming were used for kinematic analysis: of these seven were of swimming at 0.5 $L\ s^{-1}$, fourteen at 1.2 $L\ s^{-1}$, and twelve at 2.0 $L\ s^{-1}$. These speeds were specifically chosen to cover the range of natural locomotor behaviors in bluegill sunfish (Drucker, 1996; Drucker and Lauder, 1999; Gibb et al., 1999; Lauder, 2000). At 0.5 $L\ s^{-1}$, bluegill use slow pectoral fin swimming with little to no body undulation and only minor movements within the tail surface are occasionally visible. At 1.2 $L\ s^{-1}$, bluegill first begin to use regular rhythmic undulatory locomotion involving body bending (Drucker and Lauder, 2000; Gibb et al., 1999), although intermittent beats of the pectoral fins also occur. At 2.0 $L\ s^{-1}$, pectoral fin beats are infrequent, and locomotion occurs by rapid body undulation. This is near the maximal speed at which bluegill can sustain undulatory locomotion for 1–2 min before tiring noticeably.

Two kinematic variables were used to describe the action of the tail fin: mean lateral excursion (cm) and mean tail height (cm) measured three-dimensionally. Mean lateral excursion was defined as the average lateral distance traveled by the dorsal tip of the tail, as this was the point that moved the most and was the first part of the tail to move during lateral flexion. Mean tail height was calculated in 3D from the dorsal tip to the ventral tip of the posterior edge of the tail fin.

Electromyographic protocol

Bluegill were anaesthetized using tricaine methanesulfonate (MS222) buffered with potassium hydroxide and actively ventilated using water oxygenated by an aquarium air pump throughout the procedure, as in previous research (Jayne and Lauder, 1993; Jayne et al., 1996; Tytell and Lauder, 2002). Fish were allowed to recuperate fully from the anesthesia following electrode insertion before any swimming procedures were begun. As a general rule, fish were fully recuperated after twice the time that they were under anesthesia had passed.

Electrodes were made from 2 m lengths of 0.05 mm diameter bifilar Teflon-coated steel wire (California Fine Wire Co., Grover Beach, CA, USA). The wires were split apart along 1 mm of their long axis and 0.5 mm of the tip of one wire was removed, so that the tips did not contact each other. The insulation was removed from a 0.5 mm section at the tip of each wire, and the electrode tips was bent back into a hook shape. Electrodes were threaded through a 26-guage needle for subcutaneous surgical implantation into the fish muscle. Care was taken to standardize electrode construction in order to minimize signal variation.

Electrodes were placed bilaterally in a total of 24 muscles of the caudal peduncle and fin (13 muscles maximum per experiment) to account for any local muscle activity contributing to tail shape. Muscles studied included the flexor dorsalis (FD), flexor ventralis (FV), hypochordal longitudinalis (HL), infracarinalis posterior (IC), nine of the interradialis (IR) muscles, of which there are 32 in total between all the caudal fin rays, lateralis superficialis (LS) in the caudal peduncle, dorsal to the lateral red muscle, supracarinalis posterior (SC), and the lateral red muscle in the myotomes just anterior to the caudal peduncle (Fig. 1). The electrodes in the caudal peduncle red fibers correspond in placement to position 7 of Jayne and Lauder (Jayne and Lauder, 1995a) (Fig. 1). Electrodes were inserted on both the left and right sides of the fishes to include activity throughout an entire tail beat and to minimize the chance that fish would favor one side.

Electromyographic signals were amplified by a factor of 5000 using Grass model P511 K amplifiers with high- and low-bandpass filter settings of 100 Hz and 3 kHz, respectively, and a 60 Hz notch

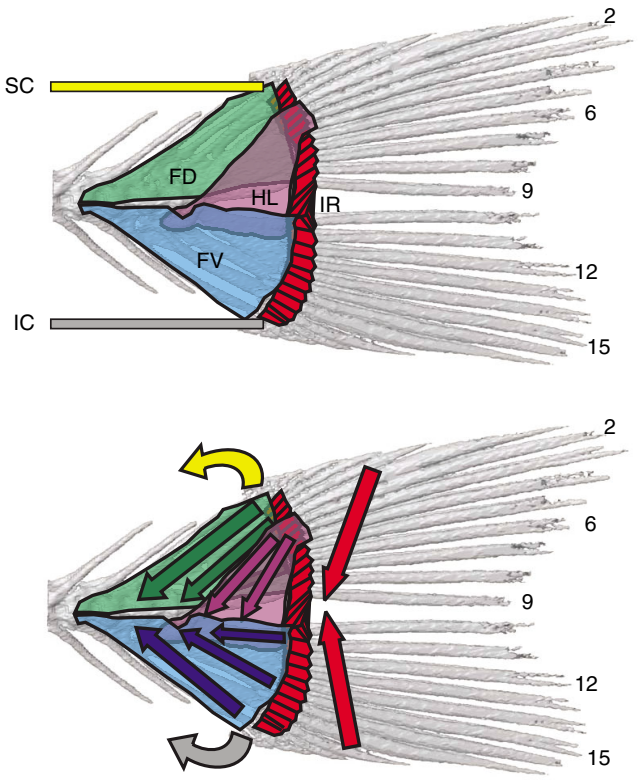

Fig. 1. Anatomy of intrinsic caudal muscles, overlaid on a computer microtomography (μCT) scan of a bluegill sunfish tail. Arrows in the bottom diagram indicate the direction of movement of fin components caused by muscle contraction as determined from electrical stimulation experiments. FD, flexor dorsalis; FV flexor ventralis; HL, hypochordal longitudinalis; IC, infracarinalis; IR, interradialis, designated by fin ray position; SC, supracarinalis. The fin rays are numbered dorsal to ventral. Not depicted in this diagram are the lateralis superficialis (LS) and lateral muscle band of the axial myomeres, which lie superficially to the intrinsic caudal muscles pictured above.

filter. Electromyograms were recorded digitally using an ADInstruments PowerLab/16SP analog-to-digital converter and Chart 5.4.2 software (ADIntruments, Inc., Colorado Springs, CO, USA) at a sampling rate of 4 kHz. Electromyographic signals were recorded for a total of five fish, with electrodes implanted in 13 muscles at a time, swimming steadily at 0.5, 1.2, and 2.0 $L\ s^{-1}$ for a minimum of five consecutive tail beats at each speed. The number of individuals and tail beat sequences at each speed for which muscle activity was recorded is summarized in Table 1. Following recordings, fish were anaesthetized and fixed. Electrodes were then dissected out to verify placement.

Electrical stimulation experiment

Electrical stimulation was performed to initiate contraction and elucidate the function of each intrinsic tail muscle individually. For the purpose of the electrical stimulation experiments, a lethal dose of MS222 was administered to one fish. The skin over the tail was then removed to visually ensure direct electrode placement in the correct muscles. Electromyographic electrodes were implanted into the flexor dorsalis (FD), flexor ventralis (FV), hypochordal longitudinalis (HL), infracarinalis posterior (IC), interradialis (IR) between each of the caudal fin rays, lateralis superficialis (LS), and supracarinalis posterior (SC) muscles to determine what their action upon activation might be. The free ends of the electrodes were attached to a Grass S44 electrical stimulator, and muscles were stimulated both separately and in groups at 10–20 V for 1 s duration of 10–30 pulses s^{-1} with a 1 ms delay between pulses. A video camera (Sony Digital Handycam DCR-TRV38) was mounted above the fish tail during the stimulation experiment to capture caudal fin movement for later analysis.

Data analysis

Electromyographic recordings that corresponded with clear video views of the caudal fin in all three video cameras simultaneously were used for analysis of the muscle activity. The EMG results were rectified, integrated and digitized in Chart 5.4.2 software. We recorded the onset, duration, and the intensity of each selected section of muscle activity during steady swimming sequences, where intensity was defined as the area of the integrated EMG burst.

In an effort to maximize the total number of muscles studied by electromyography, and since we were limited by the equipment to simultaneous recording of only 13 electrodes in any one fish, many of the specific muscles examined were different for each individual and a few of the implantations were not successful. In all individuals, the activity of the red muscle along the midline of the caudal peduncle and the hypochordal longitudinalis (HL) were recorded, and the activity of all other muscles in each fish was analyzed relative to these shared muscles. Owing to the number of muscles studied within the tail and the fact that some recordings from individual muscles did not yield analyzable data, the final data set had missing recordings for different muscles in each of the different individual fish. As a result of the pattern of missing values, it was not possible to perform a single global analysis of variance (ANOVA) amongst all individuals, muscles, and swimming speeds. Analysis of variance of duration and intensity of activity of muscles shared amongst individuals and swimming speeds, where each muscle was recorded in at least three individuals at each speed, showed that there was no significant difference among individuals (F_{ANOVA}=0.2662, $F_{0.05(1),11,24}$=2.22, P>0.25; power=0.878). Therefore, there was only a 12% chance that individuals were different, and so one-way ANOVAs were used to compare muscle activity duration, relative onset of muscle activity, and EMG burst duration by muscle. In addition, principal component analysis (PCA) was implemented on muscle activity duration, relative onset of muscle activity, and EMG burst duration data of each muscle pooled by swimming speeds.

RESULTS

Muscle anatomy

The intrinsic caudal musculature of *Lepomis macrochirus*, as seen in Fig. 1, is generally similar to that described previously in other euteleost fishes (Lauder, 1982; Winterbottom, 1974). The flexor dorsalis (FD) originates on the dorsal and lateral aspect of the last few vertebral centra, neural spines and upper hypurals and inserts onto the seven or eight dorsal-most fin rays. The flexor ventralis (FV) originates on the hypurapophysis, lower hypurals, and haemal spines of the posterior-most vertebrae and inserts onto the eight ventral fin rays. The hypochordal longitudinalis (HL) originates below the FV on the hypurapophysis and lower hypurals and extends posterodorsally, inserting superficially to the FD onto the four dorsal-most fin rays. The infracarinalis posterior (IC) and supracarinalis posterior (SC) are thin paired muscles located at the ventral- and dorsal-most edges of the caudal peduncle, respectively (Fig. 1). The IC originates at the posterior pterygiophore of the anal fin and inserts on the ventral-most fin ray and raylets. The SC

Table 1. Summary of electromyographic experiments

		Speed (L s^{-1})					
		0.5		1.2		2.0	
Muscle	N	Left	Right	Left	Right	Left	Right
Red lateral muscle of peduncle (RED)	5	n.a.	16	n.a.	41	n.a.	55
Hypochordal longitudinalis (HL)	5	4	4	30	30	38	37
Flexor dorsalis (FD)	4	3	4	20	24	29	25
Flexor ventralis (FV)	3	0	0	20	12	33	18
Supracarinalis (SC)	5	2	4	15	30	20	34
Infracarinalis (IC)	4	3	7	20	25	20	30
Interradialis 3 (IR3)	2	0	n.a.	10	n.a.	14	n.a.
Interradialis 6 (IR6)	4	5	n.a.	14	n.a.	19	n.a.
Interradialis 9 (IR9)	4	1	n.a.	30	n.a.	50	n.a.
Interradialis 12 (IR12)	4	9	n.a.	20	n.a.	35	n.a.
Interradialis 15 (IR15)	2	0	n.a.	10	n.a.	16	n.a.
Interradialis 5 (IR5)	2	n.a.	0	n.a.	5	n.a.	16
Interradialis 11 (IR11)	2	n.a.	0	n.a.	10	n.a.	16
Interradialis 13 (IR13)	2	n.a.	0	n.a.	10	n.a.	16
Lateralis superficialis (LS)	5	n.a.	4	n.a.	41	n.a.	55

Muscle activity recorded by electrode implantation into intrinsic caudal fin muscles, number of fish with successful implantation in each muscle, and number of tail beats analyzed for each muscle from which electrical activity was recorded at each speed. N is the number of fish for which each muscle was successfully implanted, and n.a. indicates that there was no attempt to place an electrode in that position.

originates from the posterior pterygiophore of the dorsal fin and inserts on the dorsal-most fin rays and raylets. The interradialis (IR) muscles are a series of small angled muscles found between each of the fin rays. Interradialis muscles between fin ray pairs from the first to the tenth fin rays are oriented posterodorsally, whereas IR muscles between fin ray pairs from the ninth to the seventeenth fin rays are oriented posteroventrally (Fig. 1).

Overlying the intrinsic caudal musculature in the region of the caudal peduncle are the lateralis superficialis (LS) and a thin segment of red muscle adjacent to the horizontal septum. Anterior to the caudal peduncle, the LS is a thin band of muscle positioned mediolaterally above the connection between the epaxial and hypaxial musculature. Within the caudal peduncle, however, the LS fans out posteriorly into a thin tendinous expanded sheet to cover the majority of the intrinsic caudal musculature and inserts on the caudal fin rays. Embedded superficially in this muscle, along the midline, is a thin strip of red muscle.

Electrical stimulation

The majority of intrinsic caudal muscles tested during the stimulation experiments caused lateral flexion of the tail, as well as either abduction or adduction of the dorsal and ventral lobes of the tail fin (Table 2, Fig. 1). Lateral flexion of the tail was produced by the hypochordal longitudinalis (HL), flexor dorsalis (FD) and flexor ventralis (FV) muscles. Abduction of the fin rays, which created an increase in the surface area of the caudal fin, was accomplished by the FD, FV, supracarinalis (SC) and infracarinalis (IC) muscles. Reduction in the surface area of the fin occurred through adduction of the fin rays by the contraction of the HL and interradialis muscles (IR). When stimulated, the IR muscles acted only on the fin rays to which they were inserted; they did not affect other sections of IR muscles or fin rays elsewhere in the fin. Simultaneous stimulation of the FD and SC muscles caused greater abduction of the dorsal fin rays than either muscle had caused independently. Also, simultaneous stimulation of the FD, FV, SC and IC induced greater abduction of the fin rays than stimulations of the FD and FV or SC and IC had caused.

Overview of recruitment pattern

Fish swimming steadily while the speed of the water in the flow tank was slowly increased from 0 to 2.0 L s^{-1} exhibited both changes in the timing and burst intensity of the electromyographic recordings (Fig. 2). Initially, at zero flow, no intrinsic caudal fin muscles were active. As flow speed increased to near 0.5 L s^{-1}, low

Table 2. Results of *in situ* stimulation experiment on intrinsic caudal musculature of *Lepomis macrochirus*

Muscle activated	Action observed
Hypochordal longitudinalis (HL)	Adduction and lateral flexion of dorsal lobe (fin rays 1–4)
Flexor dorsalis (FD)	Abduction and lateral flexion of dorsal lobe (fin rays 1–3)
Flexor ventralis (FV)	Abduction and lateral flexion of ventral lobe (fins rays 10–17)
Supracarinalis (SC)	Dorsal rotation of caudal peduncle and fin, abduction of raylets and first fin ray of dorsal lobe
Infracarinalis (IC)	Ventral rotation of caudal peduncle and fin
Interradialis 5 (IR5)	Adduction of the fifth fin ray towards midline
Interradialis 9 (IR9)	Adduction of the ninth and tenth fin rays towards midline
FD + FV	Abduction of dorsal and ventral fin rays, some lateral flexion
FD + SC	Abduction dorsal fin rays and lateral flexion
SC + IC	Abduction of dorsal and ventral lobes of fin
FD + FV + SC + IC	Abduction of dorsal and ventral lobes and lateral flexion of the fin

Pulses of 10–20 V were applied at a rate of 10–30 pulses s^{-1}, with a 1 ms delay between pulses, for 1 s duration.

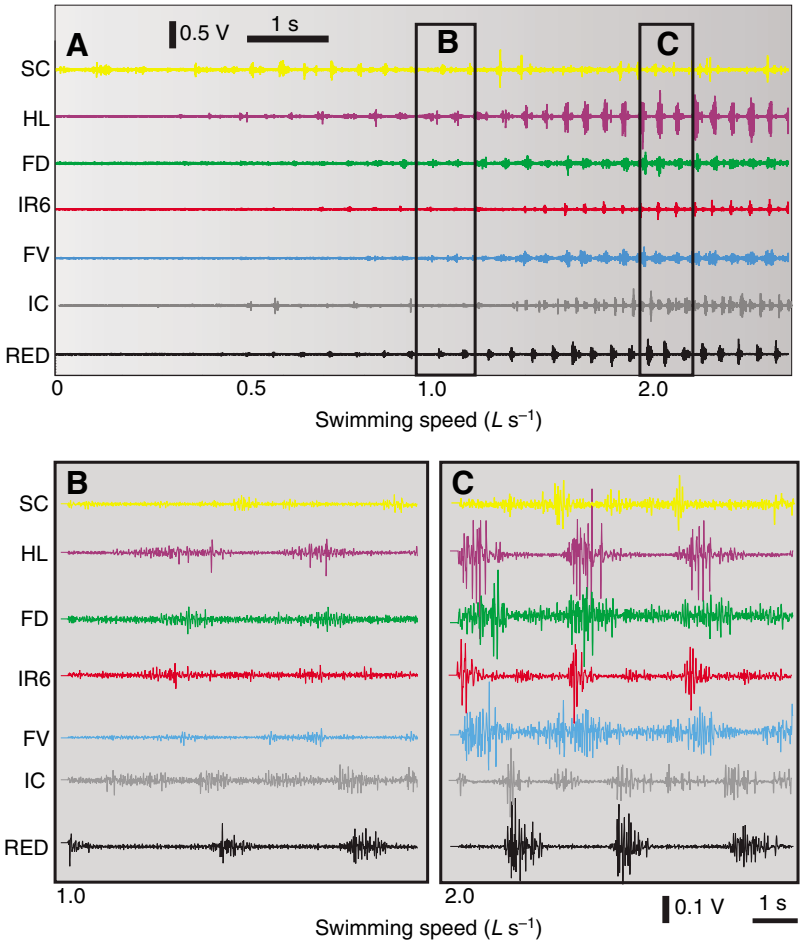

Fig. 2. (A) Electromyographic sequence (amplified 5000×) of a bluegill sunfish (*Lepomis macrochirus*) swimming while the speed of the flow tank was gradually increased from swim speeds of 0 to 2.0 $L\ s^{-1}$. Muscle activity is shown for the supracarinalis (SC), hypochordal longitudinalis (HL), flexor dorsalis (FD), interradialis (IR) designated by the number of its dorsally corresponding fin ray, and flexor ventralis (FV) on the left side, and the infracarinalis (IC) and red myomere (RED) on the right side of the fish. (B,C) Enlarged subset of sequences of fish swimming at 1.0 (B) and 2.0 (C) $L\ s^{-1}$. The scale for sequences B and C is in the lower right corner below C. EMG color corresponds to the anatomical diagram in Fig. 1.

amplitude irregular rhythmic bursting in some intrinsic muscles was observed (Fig. 2A), and similar very low amplitude activity was seen in the posterior red fibers in the caudal peduncle. As flow speed increased to near 1.0 $L\ s^{-1}$, higher amplitude bursts were observed in all muscles (Fig. 2B). At higher speeds approaching 2.0 $L\ s^{-1}$, duration of muscle bursts decreased while the overall magnitude of the recorded bursts, or intensity, increased dramatically (compare Fig. 2B and C). Not all muscles initiated activity at the same speed: the supracarinalis (SC), hypochordal longitudinalis (HL), infracarinalis (IC), and red lateral muscle were occasionally active at speeds lower than 0.5 $L\ s^{-1}$ whereas other intrinsic muscles were not active until the fish approached speeds of 1.2 $L\ s^{-1}$.

Kinematic and EMG analysis

Fish swimming at 0.5 $L\ s^{-1}$ primarily used their pectoral fins for locomotion; therefore only minor tail fin movements and shape modulation were observed at this speed (Fig. 3). Mean lateral excursion of the tail was less than 0.25 cm from the median axis of the fish and maximum excursion occurred at approximately 10 and 55% of the tail beat cycle. The average duration of the tail beat cycle, as determined by onset of red axial myomere activity, was 0.47 s (N=16). Mean tail height was generally between 4.6 and 4.9 cm from the dorsal tip to the ventral tip of the tail. Low amplitude, sustained ipsilateral activity of the supracarinalis (SC), hypochordal longitudinalis (HL), flexor dorsalis (FD) and infracarinalis (IC) muscles occurred throughout the nominal flexion of the tail. Only two fish exhibited interradialis (IR) muscle activity at this speed. The IR6 muscle was active at a different proportion of the tail beat cycle for each of the five sequences in which it was active. Out of phase muscle activity by the left IR12 that occurred in the first 15% of the tail beat occurred during four sequences from the same fish at 0.5 $L\ s^{-1}$; no other fish demonstrated this muscle activity and it was most likely a result of the electrode initially being inserted too deeply and contacting the right IR12 but later being pulled during swimming into the left IR12, where placement was confirmed post-mortem.

Tail fin muscle activation and fin shape modulation increased greatly during locomotion at 1.2 $L\ s^{-1}$ (Fig. 4). Mean lateral excursion of the tail increased 400%, to 1.0 cm from the median axis, and was significantly different from fish swimming at 0.5 $L\ s^{-1}$ ($t_{0.05(2),6}$; P<0.001). Maximum lateral excursion of the tail occurred at approximately 15% and 65% of the tail beat cycle. The average duration of a tail beat at 1.2 $L\ s^{-1}$ was 0.25 s (N=45). Mean tail height was between 5.5 and 5.9 cm, a 1 cm (20%) increase in tail height as compared to swimming at 0.5 $L\ s^{-1}$. Maximum tail height occurred at about 35% of the tail beat cycle, prior to when the tail was midway between maximal lateral excursion, as it crossed the median plane. Minimum tail height occurred at about 10% and 65% of the tail beat cycle, just after points of maximum excursion. At that time, both the SC and IC muscles of the left and right sides were active. Interradialis muscle activity was also initiated at 1.2 $L\ s^{-1}$, with the dorsal-most IR muscles active first and muscle activity onset proceeding ventrally. Simultaneous contralateral activity of the IR muscles occurred at 55% of the tail beat cycle, just before maximum excursion.

As fish swimming speed increased from 1.2 $L\,s^{-1}$ to 2.0 $L\,s^{-1}$, more changes occurred in tail beat amplitude and relative timing of kinematic variables (Fig. 5). There was a significant decrease in mean lateral excursion to 0.65 cm when swimming speed increased to 2.0 $L\,s^{-1}$ ($t_{0.05(2),6}$; $P<0.001$). Time of the average tail beat was 0.19 s (N=55). Mean tail fin height appeared to fluctuate more rapidly but remained within 5.3 to 5.8 cm, showing no consistent pattern of change in height from swimming at 1.2 $L\,s^{-1}$; however maximum tail height was reached at 45% of the tail beat cycle and minimum tail height was at 20 and 70% of the tail beat cycle. At 2.0 $L\,s^{-1}$, minimum tail height coincided with the dorsal tail tip being at maximum lateral excursion. Both the SC and IC muscles of the left and right sides showed considerable overlap in activity patterns, coinciding with the tail being 65% between points of maximum excursion and with greatest tail height. Again, the IR muscles were activated sequentially from dorsal-most to ventral-most, and simultaneous contralateral activity occurred at 50% of the tail beat cycle. The lateralis superficialis (LS) muscles were activated in an anterior to posterior pattern. Overall, the activity of the muscles within the caudal peduncle originated anteriorly near the dorsal and ventral edges of the peduncle, progressed towards the midline, and then posteriorly towards the caudal fin.

Muscle activity duration and burst intensity changed with increasing speed; however, the relative time of onset of muscle activity showed no relationship with swimming speed (Fig. 6). The duration of muscle activity decreased with increasing swim speed from 0.5 $L\,s^{-1}$ to 1.2 $L\,s^{-1}$, decreasing by 50–70% in the cases of the red myomere, HL, FD, SC, IC and LS muscles. However, none of the muscles, with the exception of IR3, had a significant change in muscle activity duration when swimming speed was increased from 1.2 $L\,s^{-1}$ to 2.0 $L\,s^{-1}$. Thus, muscles were active for a greater proportion of the tail beat cycle at 2.0 $L\,s^{-1}$. There was no

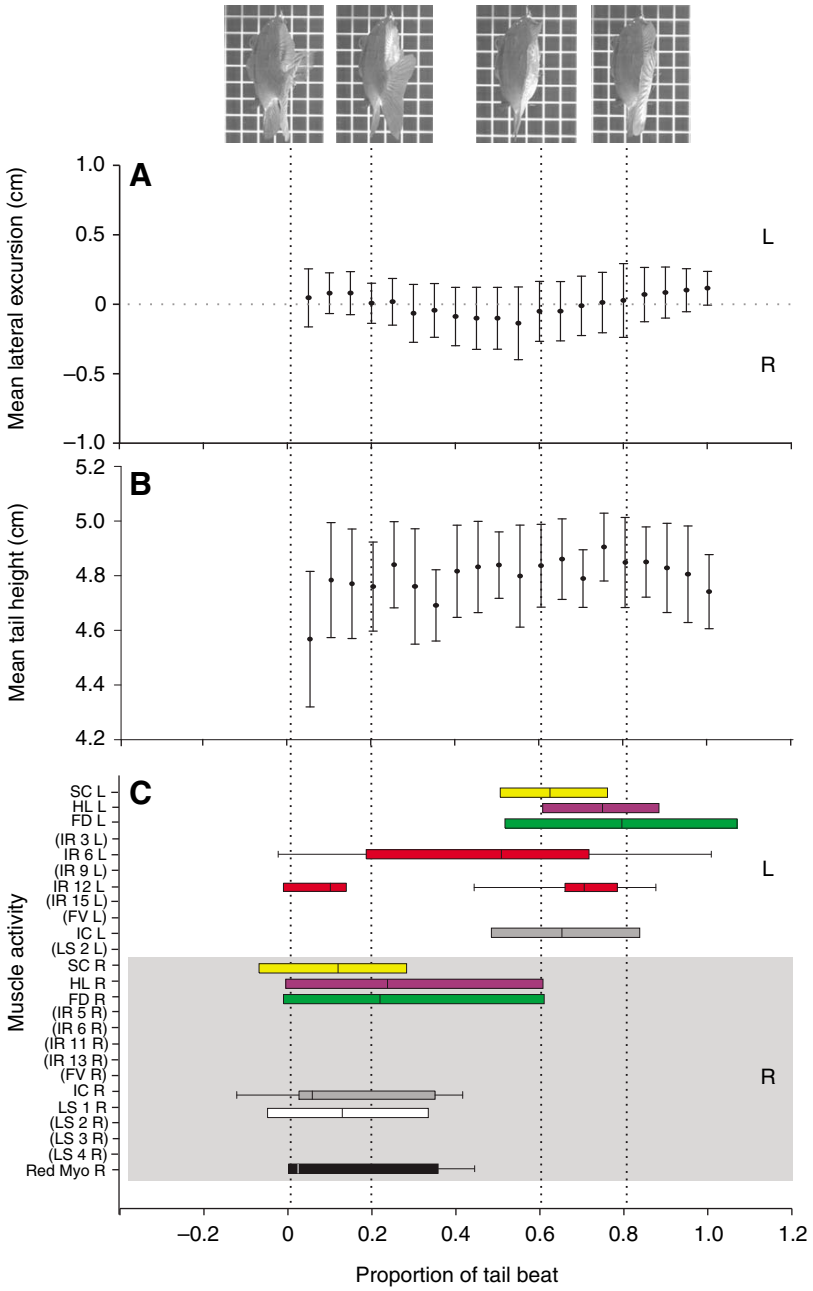

Fig. 3. Posterior view of fish (images above plot), mean lateral excursion of tail fin (A), mean tail fin height (B), and activity of intrinsic caudal muscles (C) throughout one tail beat during steady swimming at 0.5 $L\,s^{-1}$ (N=7 tail beats). Lateral excursion and tail height are plotted as mean (circles) ± s.e.m. Colored horizontal bars denote muscle activity within 75% confidence interval (CI) and error bars denote the 95% CI. Parentheses around muscle names indicate muscles inactive at this swimming speed. Muscle activity is shown for the left (L) and right (R) sides; supracarinalis (SC), hypochordal longitudinalis (HL), flexor dorsalis (FD), interradialis (IR) designated by the number of the dorsally corresponding fin ray, flexor ventralis (FV), infracarinalis (IC), lateralis superficialis (LS), and red myomere on the right side of the caudal peduncle. Dotted vertical lines indicate the times of each image at the top. Bar color corresponds to the anatomical diagram in Fig. 1.

significant difference in relative time of muscle onset among swimming speeds. Increasing swimming speed resulted in increases of 50–100% of muscle burst intensity. In particular, the burst intensity of the HL, FD, FV, SC, IC and IR9 increased significantly with each speed transition. Analysis of variance determined that muscle activity duration and burst intensity were significantly different amongst all speeds and muscles ($F_{0.05(1),35,536}$=1.42, P<0.001).

Principal component analysis of the duration of muscle activity, relative time of onset, and intensity of EMG burst for each muscle determined that three factors explained 54% of the total variance (82% of the total variance was attributed to seven discrete factors within the data; Fig. 7). Factor one, which described 25% of the variation, separated the data by speeds and represented an inverse relationship in duration of muscle activity and intensity of EMG burst, where positive values represented an increase in duration and a decrease in intensity and negative numbers represented a decrease in duration and an increase in intensity. Factor two described 17% of the variance and separated the ventral IR muscles (negative components) from the red and dorsal IR muscles (positive components) at 1.2 L s^{-1}. The third factor described only 12% of the variance, but separated the IR muscles (positive components) from all other muscles studied (negative components).

DISCUSSION

The intrinsic caudal muscles of teleost fishes are derived from the posterior-most axial body musculature (Gemballa, 2004; Videler, 1975; Winterbottom, 1974); however, they differ greatly in both morphology and function. The posterior vertebral processes and the uroneural and hypural bony elements in the tail are modified into broad, laterally compressed plates from which the intrinsic caudal

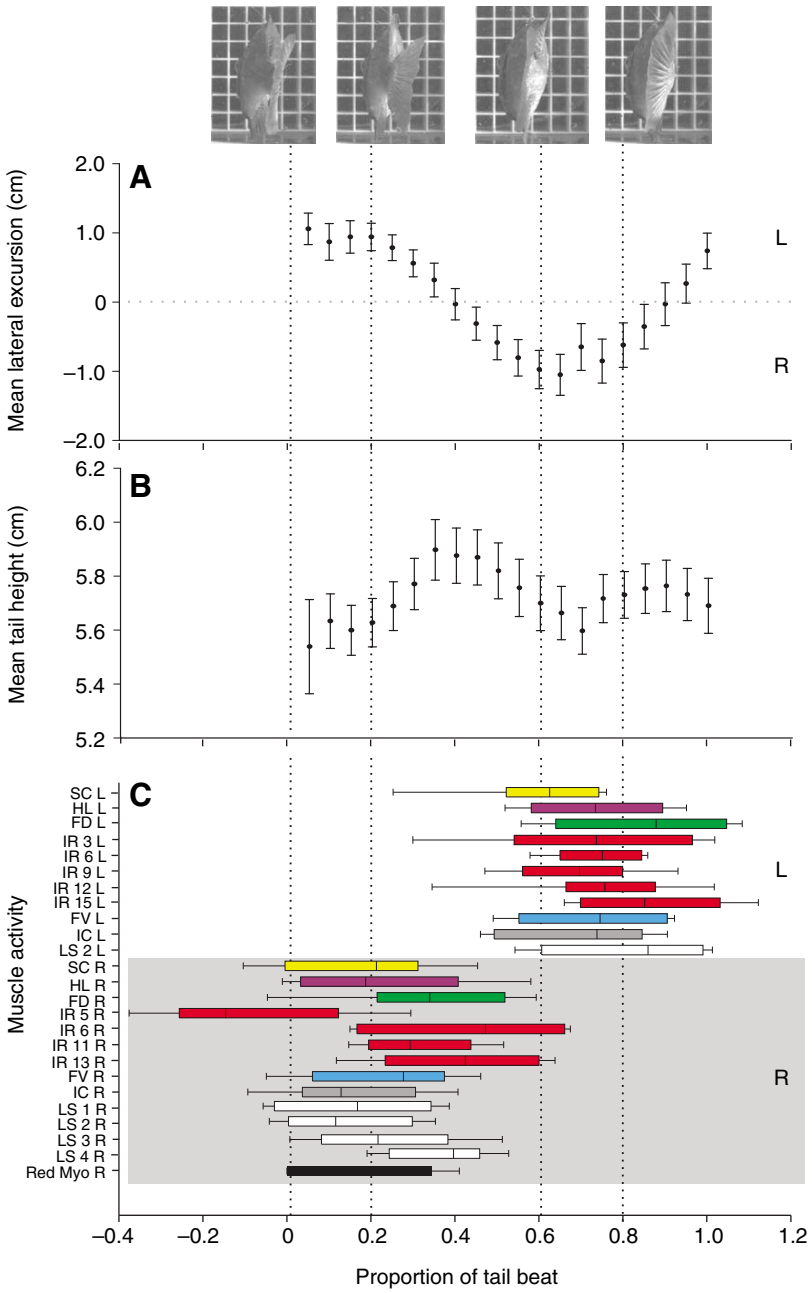

Fig. 4. Posterior view of fish (images above plot), mean lateral excursion of tail fin (A), mean tail fin height (B), and activity of intrinsic caudal muscles (C) throughout one tail beat during steady swimming at 1.2 L s^{-1} (N=14). Lateral excursion and tail height are plotted as mean (circles) ± s.e.m. Colored horizontal bars denote muscle activity within 75% confidence interval (CI) and error bars denote the 95% CI. Muscle activity is shown for the left (L) and right (R) sides; supracarinalis (SC), hypochordal longitudinalis (HL), flexor dorsalis (FD), interradialis (IR) designated by the number of the dorsally corresponding fin ray, flexor ventralis (FV), infracarinalis (IC), lateralis superficialis (LS), and red myomere on the right side of the caudal peduncle. Dotted vertical lines indicate the times of each image at the top. Bar color corresponds to the anatomical diagram in Fig. 1.

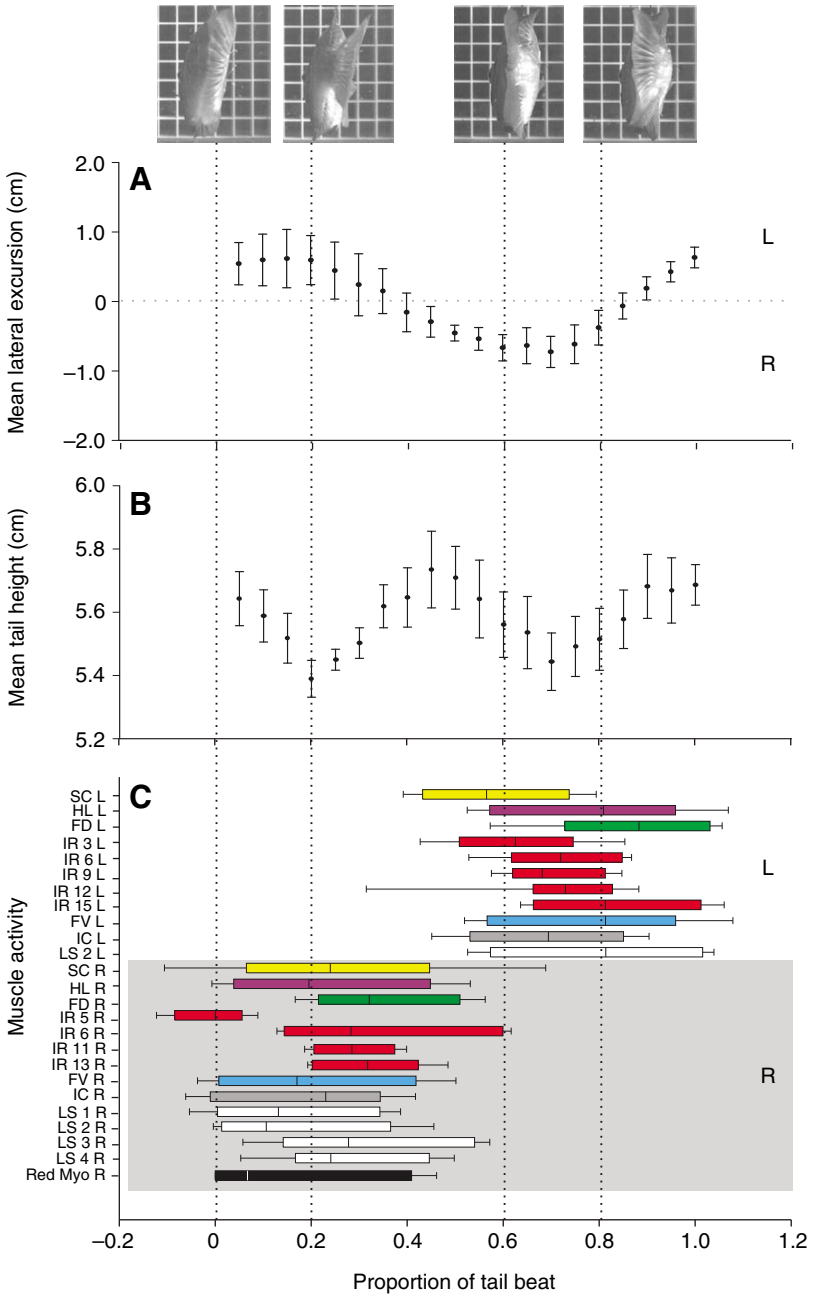

Fig. 5. Posterior view of fish (image above plot), mean lateral excursion of tail fin (A), mean tail fin height (B), and activity of intrinsic caudal muscles (C) throughout one tail beat during steady swimming at 2.0 $L\ s^{-1}$ (N=12). Lateral excursion and tail height are plotted as mean (circles) ± s.e.m. Colored horizontal bars denote muscle activity within 75% confidence interval (CI) and error bars denote the 95%CI. Muscle activity is shown for the left (L) and right (R) sides; supracarinalis (SC), hypochordal longitudinalis (HL), flexor dorsalis (FD), interradialis (IR) designated by the number of the dorsally corresponding fin ray, flexor ventralis (FV), infracarinalis (IC), lateralis superficialis (LS), and red myomere on the right side of the caudal peduncle. Dotted vertical lines indicate the times of each image at the top. Bar color corresponds to the anatomical diagram in Fig. 1.

muscles originate (Lauder, 1989; Lauder, 2000; Lauder and Liem, 1983; Liem, 1970; Nag, 1967; Videler, 1975; Winterbottom, 1974). Posteriorly, the fin rays, or lepidotrichia, rest on the distal edge of the uroneurals and hypurals and form the flexible caudal foil. The lepidotrichia are modified scale rows (Eaton, 1945; Videler, 1975) deep to the intrinsic musculature that inserts onto the rays and controls their movement. Fish fin rays possess a remarkable bilaminar structure that permits musculature attachment to the two heads of the half rays (termed hemitrichs) to actively control the curvature of the fin rays (Alben et al., 2007; Geerlink and Videler, 1987; Lauder et al., 2006). Control of caudal fin curvature and stiffness thus could be accomplished by activity of intrinsic tail muscles. Low amplitude thrust forces could also be generated by alternating activation of intrinsic tail muscles, causing the caudal fin rays to oscillate at low speeds where there is no active body undulation.

Lateral flexion of fin rays is controlled through the relatively large hypochordal longitudinalis (HL), flexor dorsalis (FD) and flexor ventralis (FV) muscles. Collectively, these muscles insert onto the lateral aspects of all the fin rays; in the case of the four dorsal-most fin rays, both the HL and FD cause lateral flexion. The supracarinalis posterior (SC) and infracarinalis posterior (IC) muscles, in conjunction with the FD and FV muscles, are primarily responsible for the dorsoventral abduction of fin rays from the midline. Adduction of the fin rays towards the midline is accomplished by the interradialis muscles.

Speed effects on intrinsic tail muscle recruitment

Intrinsic caudal fin muscles are active from the very beginning of undulatory locomotion and even, intermittently, at speeds associated with paired fin locomotion (Drucker and Lauder, 1999; Gibb et al., 1994) where the body does not undergo

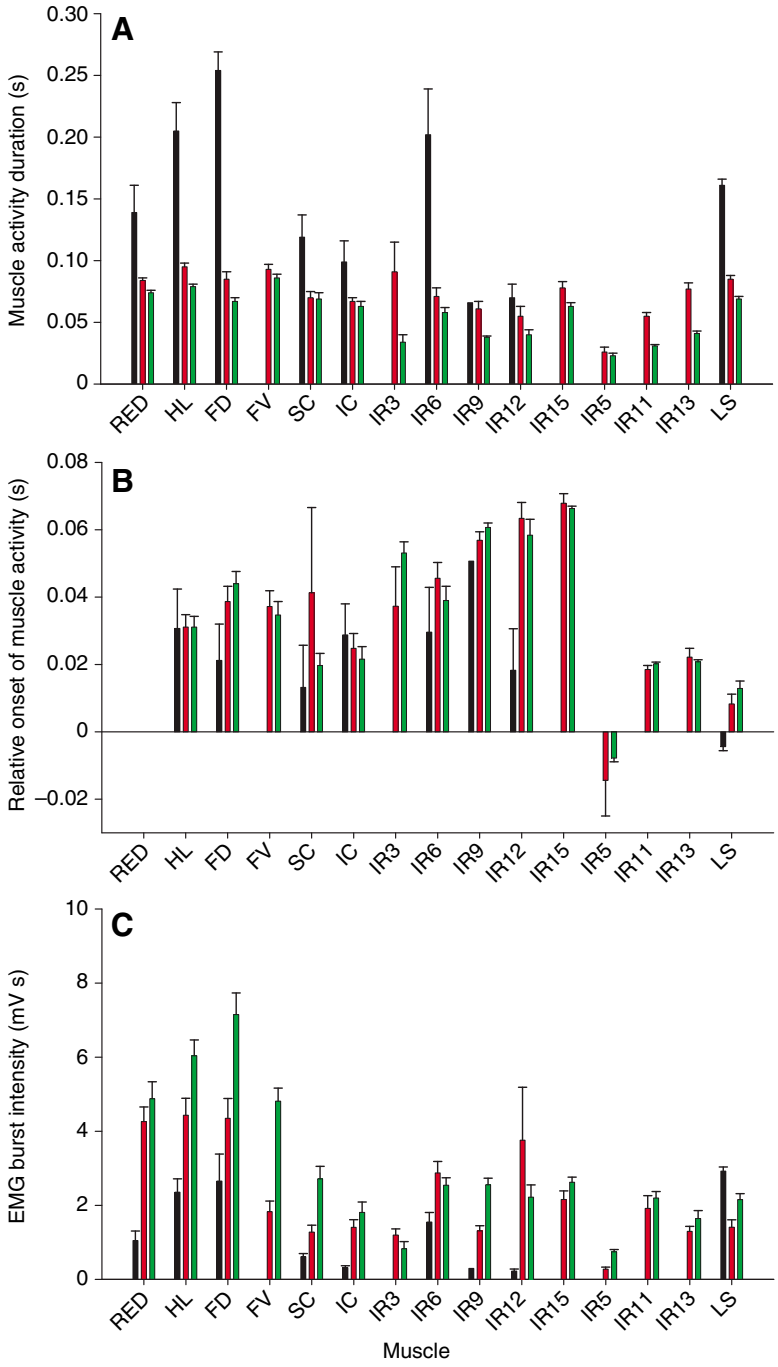

Fig. 6. Histograms of muscle activity duration (A), onset of muscle activity relative to lateral red muscle onset (B), and EMG burst intensity (C) of intrinsic caudal muscles on the right side at 0.5 (black bars), 1.2 (red bars), and 2.0 $L\ s^{-1}$ (green bars). Error bars indicate standard error of the mean. Muscle activity is shown for the red myomere (RED), hypochordal longitudinalis (HL), flexor dorsalis (FD), flexor ventralis (FV), supracarinalis (SC), infracarinalis (IC), interradialis (IR) designated by the number of the dorsally corresponding fin ray, and lateralis superficialis (LS). Some muscles were not active at 0.5 $L\ s^{-1}$ (e.g. FV) and therefore a gap is present instead of a black bar.

rhythmic oscillatory patterns. Even at slow speeds between 0.5 and 1.2 $L\ s^{-1}$ where complex conformational changes of the tail do not occur, some intrinsic tail muscles are active, and as speed increases all intrinsic muscles are strongly activated. We found no intrinsic muscles that remained inactive during steady swimming once speeds above 1.0 $L\ s^{-1}$ were achieved. This result indicates that of all muscle fibers activated by the spinal cord during locomotion, the intrinsic tail muscles, innervated by the most posterior spinal neurons, are the first to be recruited. This recruitment occurs even prior to activation of most of the red muscle fibers in myotomes anterior to the caudal peduncle.

The timing of intrinsic caudal muscle activity during the tail beat corresponded with the caudal fin kinematics measured. Little to no intrinsic caudal muscle activity was detected below 0.5 $L\ s^{-1}$, corresponding with the low amplitude caudal fin motion. Electrical activity identified in the HL, FD, IC and SC muscles at 0.5 $L\ s^{-1}$, which co-occurred with minimally noticeable effect on tail fin kinematics, may act instead to stiffen the tail; as bluegill sunfish generally swim with only its pectoral fins at this speed (Gibb et al., 1994; Webb, 1973). Stiffening of the caudal fin *via* low intensity activity in these intrinsic muscles may aid in drag reduction by minimizing tail motion caused by the wake produced by upstream median and paired fins (Tytell, 2006). Sunfish, as well as other fishes, tend to cup the dorsal and ventral edges of their caudal fin into oncoming flow at moderate steady swimming speeds (Bainbridge, 1963; Lauder, 2000; Tytell, 2006), an action that would be caused by activation of the HL, FD, IC and SC muscles.

The timing of the activity of these muscles was synchronous with the caudal fin being slightly cupped to the ipsilateral side, and lateral fin cupping is most likely caused by the activity of these intrinsic muscles.

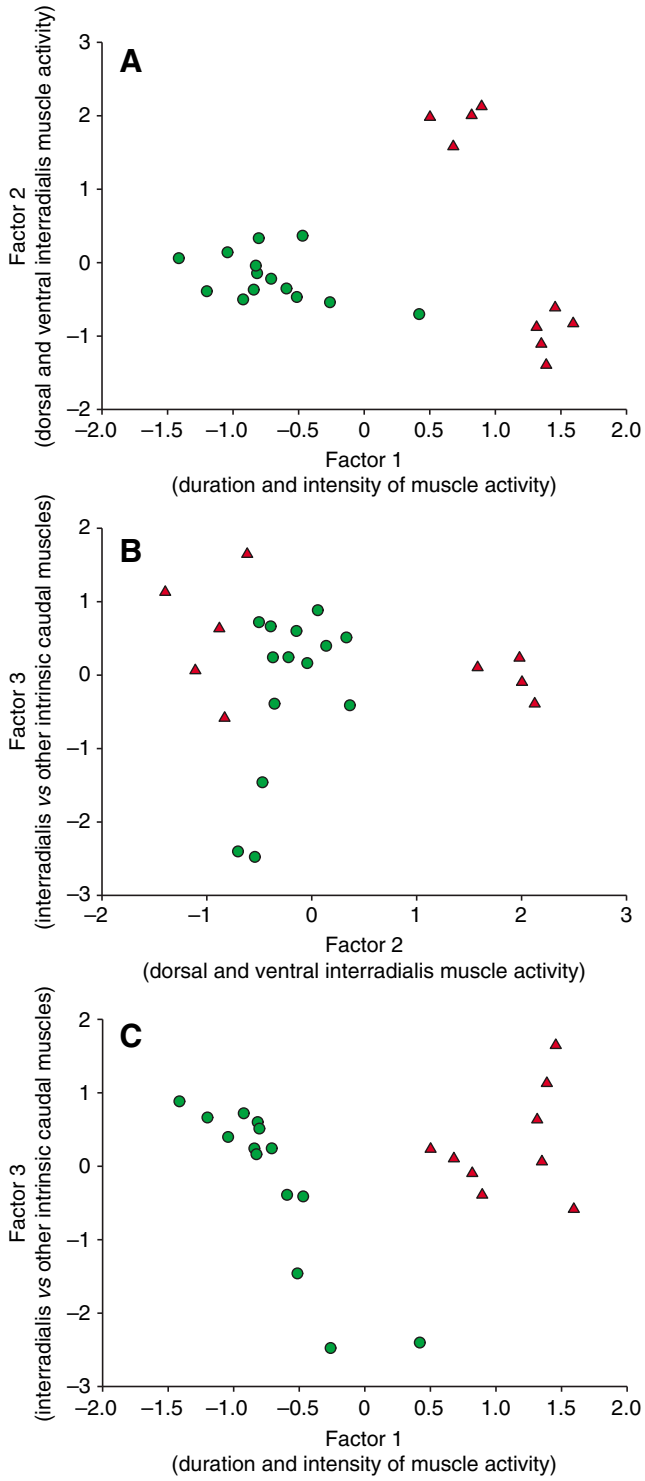

Fig. 7. Principal component analysis of muscle activity duration, relative onset of muscle activity and EMG burst intensity for fish swimming at 1.2 $L\,s^{-1}$ (red triangles) and 2.0 $L\,s^{-1}$ (green circles). Each point represents one measurement of muscle activity over one tail beat cycle. A description of the variable types loading heavily on each factor is given below the axis label. Further explanation of factor loadings is given in the text.

At higher swim speeds of 1.2 and 2.0 $L\,s^{-1}$, more muscles are involved in complex activity patterns as tail shape modulation increases compared with swimming at 0.5 $L\,s^{-1}$ (Fig. 4). Muscle activity patterns at these two higher swim speeds is very similar in many regards. At both 1.2 and 2.0 $L\,s^{-1}$, there was a great deal of contralateral overlap of muscle activity at points of maximum tail excursion. Overall, activity of all intrinsic muscles on each side of the tail showed a high degree of overlap, and only a few interradialis muscles exhibited substantial differences in activity from the other intrinsic caudal muscles. Electromyography detects electrical activity of muscles, which is not necessarily indicative of muscle contraction as muscles can also be electrically active when stretched. Simultaneous electrical activity on contralateral sides at maximum excursion may indicate preloading of the ipsilateral muscles just prior to their contraction, as the caudal fin changes direction and begins to move to that side. The occurrence of EMG activity during muscle lengthening secondary to contralateral activation suggests that force enhancement by pre-stretching the muscle may be used. An additional possibility is that the contralateral activity serves to stiffen the caudal fin by pulling on both hemitrichs of the caudal fin rays as the tail changes direction at maximum excursion.

Alternatively, contralateral co-activation of fin muscles may help to increase the area of the caudal fin, thereby increasing the added mass and the force created as a result of an acceleration reaction (Daniel, 1984; Denny, 1990). Contralateral overlap of the IC and SC muscles occurred at the midpoint between points of maximum excursion, as the caudal fin passed behind the body of the fish. The direct result of these muscles being simultaneously active on both sides was an increase in tail height. The minimum caudal fin height occurred at points of maximum excursion when the transverse velocity of the tail fin is approximately equal to zero. This is similar to what was found by Bainbridge (Bainbridge, 1963), who also determined that a 15% increase in tail height caused a 10% increase in surface area of the caudal fin and a 30% increase in tail height caused a 21% increase in surface area. The bluegill sunfish in this study had a 20% increase in caudal fin height from slow swimming at 0.5 $L\,s^{-1}$ to faster swimming at 1.2 $L\,s^{-1}$ and 2.0 $L\,s^{-1}$; this increase in tail height is coincident with greater activity of the intrinsic caudal muscles and is presumably important in maximizing surface area for thrust production.

In addition, activity of the ipsilateral FD, FV, HL, IC and SC just after maximum excursion coincided with cupping of the dorsal and ventral tips of the tail fin seen here and by Tytell (Tytell, 2006), demonstrating active modulation of the caudal fin during steady swimming. The kinematic results observed are likely counteracting passive deformation of the caudal fin by hydrodynamic forces, stiffening the fin rays on the ipsilateral side of motion, and maximizing fin area through the stroke to increase thrust as the caudal fin passes behind the fish. If so, this could reduce momentum lost at the tail tip, increasing the efficiency E of the caudal fin to 90% (Tytell, 2006).

Intrinsic caudal fin muscles also underwent a change in duty cycle with increasing swimming speed (Fig. 6), in contrast to axial body muscles which generally show no change in duty cycle with increasing speed (Coughlin, 2000; Jayne and Lauder, 1995a; Shadwick et al., 1998). There was no change in the absolute duration of muscle activity at 1.2 and 2.0 $L\,s^{-1}$ but both the amplitude and duration of the tail beat itself decreased with increasing swimming speed. This means that for a single tail beat, muscles are active for a longer proportion of the tail beat at 2.0 $L\,s^{-1}$ than at 1.2 $L\,s^{-1}$. As a result of increased muscle activity duration,

more muscles are active at the same time, possibly acting synergistically, increasing force production and, potentially, power output and tail stiffness.

Muscle and fiber type recruitment

The increase in EMG burst intensity with increasing swim speed suggests that a greater number of muscle fibers, perhaps even of different fiber types, are active at higher speeds. Fish muscles are composed of fibers of different metabolic types and these muscle fibers are activated at different swimming speeds (Bone, 1978; Coughlin and Rome, 1996; Jayne and Lauder, 1995b; Rome et al., 1988; Rome et al., 1993; Syme, 2006). Although a great deal of research has been conducted on myotomal muscle fiber development, anatomy and function, only one study, to our knowledge, has characterized fiber types in intrinsic caudal fin and posterior caudal peduncular muscles (Nag, 1972).

Nag (Nag, 1972) studied rainbow trout (*Salmo gairdneri*) and showed that intrinsic caudal muscles such as the superficial and deep flexor dorsalis and ventralis, hypochordal longitudinalis, and interradialis muscles all possess both red and white muscle fibers. He made no mention of any spatial segregation of fiber types within these muscles, and so we believe that each of these individual muscles in bluegill most likely has a mixed fiber population more characteristic of mammalian muscle than the spatially segregated fiber type distribution characteristic of myotomal musculature. Nag (Nag, 1972) did note that the caudal peduncle in rainbow trout possessed nearly 13% red fibers by weight, an amount approximately 13 times greater than that of anterior body myotomes. This is consistent with our recordings of activity in a number of regions in the caudal peduncle, and with the onset of electrical activity even at rather low swimming speeds when there is effectively no anterior body oscillation and only minor movement of the tail. In particular, the lateralis superficialis muscle (LS), which is often presumed to be composed of only white muscle, may in fact also contain considerable numbers of red muscle fibers, as is evidenced by its activity at slow swimming speeds (Figs 3, 4). Fiber type proportions and distribution within the caudal peduncle and intrinsic caudal fin musculature could certainly be different between rainbow trout and bluegill sunfish, but Nag's (Nag, 1972) study provides the only current data on fiber type anatomy in the caudal region of fishes.

The relative proportions of slow-oxidative (red) and fast-glycolytic (white) muscle fibers increases from anterior to posterior in many fishes (Nag, 1972; Patruno et al., 1998). During larval development, the superficial monolayer of presumptive red muscle tissue in the caudal region develops independently of the deep muscle layers of the body, and is the only muscle layer found in some caudal myomeres (Nag and Nursall, 1972; Patruno et al., 1998).

Just as the relative composition of red and white muscle fibers in the axial body musculature is different than that of the posteriormost caudal regions, the increase in intensity of muscle activity with increasing speed illustrates a pattern of intrinsic caudal muscle fiber type recruitment that appears to be different from that reported in axial body musculature. Jayne and Lauder (Jayne and Lauder, 1994) proposed a model of axial body muscle activity (based on data from bluegill sunfish) in which red muscle activity predominated at slow speeds, then both red and white muscle activity increased moderately as speed increases, and finally red muscle activity decreases until white muscle fibers are the dominant active fibers. The data in our study suggest, but not conclusively so, that in the intrinsic caudal musculature, both red and white muscle fibers are active at slower swimming speeds and continue to increase in intensity to 2.0 $L\ s^{-1}$, the fastest speed at which fish could consistently swim steadily (Fig. 6). Intrinsic caudal muscles are activated with the onset of the slowest undulatory swimming speeds, and in some cases intermittent activity is seen (Figs 2, 3) even before body undulation begins and myotomal red fibers are active. We interpret this activity as functioning to stiffen the tail to minimize drag and tail flutter during pectoral fin locomotion. Although we cannot determine if specific red or white fibers within a muscle are active or not at each speed from our current data and the presumed mixed fiber population within each tail muscle, the intrinsic caudal muscles are certainly exhibiting patterns independent of, and different from, those described in the axial myomeres from which they are derived (Gemballa, 2004; Patruno et al., 1998; Videler, 1975; Winterbottom, 1974).

Prospects

This study addressed four specific issues. First, we documented activation of intrinsic tail muscles during steady locomotion, and showed that intrinsic tail muscles are active at all steady swimming speeds. Second, these muscles become active with, and in some cases prior to, the slowest undulatory swimming speeds and maintain activity, which increases in intensity as speed increases. Third, the intrinsic muscles as a group show considerable overlap in activity pattern which suggests that a major feature of intrinsic tail muscles during steady swimming is to stiffen the tail against hydrodynamic loads, perhaps using the bilaminar fin ray mechanism, and to alter tail area rhythmically during lateral caudal oscillation. Fourth, our data suggest that intrinsic caudal musculature may be recruited in a different pattern than that observed for myotomal muscle red and white fibers. Activity in the most posterior muscles in the fish body innervated by the most distal spinal nerves is the first to occur as swimming speed increases. This indicates that at least at the slowest swimming speeds, undulatory locomotion is powered by posterior musculature, and not by anterior myotomal muscles where strains during slow swimming approach zero (Jayne and Lauder, 1995b).

The experiments described here focused on steady swimming, but of equal interest is the possible role of intrinsic tail musculature in maneuvering locomotion. This paper also does not address the fiber type distribution within intrinsic tail muscles in fishes, about which adequate data are not currently available. Also of considerable further interest is understanding the central spinal connections and projections to the intrinsic musculature of the caudal fin. How do spinal motor neurons that drive intrinsic caudal muscles connect centrally, and how do these connections compare with central myotomal projections from red and white fibers (Liu and Westerfield, 1988; McLean et al., 2007)? There is currently very little information on intrinsic caudal muscle physiology and neuroanatomy in fishes, and yet progress in this area is of considerable importance for understanding the diversity of caudal fin morphology and control in fishes, and the recruitment of muscle to power swimming.

We are grateful to Sarah Kennifer and Autumn Bonnema for assistance in conducting the experiments, to Tony Julius for fish care and maintenance, and to the Lauder lab members for input on earlier versions of this manuscript. Funding for this research was provided by NSF grant IBN0316675 to G.V.L.

REFERENCES

Alben, S., Madden, P. G. A. and Lauder, G. V. (2007). The mechanics of active fin-shape control in ray-finned fishes. *J. R. Soc. Interface* **4**, 243-256.

Bainbridge, R. (1963). Caudal fin and body movement in the propulsion of some fish. *J. Exp. Biol.* **40**, 23-56.
Bone, Q. (1978). Locomotor muscle. In *Fish Physiology: Locomotion*. Vol. VII (ed. W. S. Hoar and D. J. Randall), pp. 361-424. New York: Academic Press.
Breder, C. M. (1926). The locomotion of fishes. *Zoologica* **4**, 159-297.
Coughlin, D. J. (2000). Power production during steady swimming in largemouth bass and rainbow trout. *J. Exp. Biol.* **203**, 617-629.
Coughlin, D. J. and Rome, L. C. (1996). The roles of pink and red muscle in powering steady swimming in Scup, *Stenotomus chrysops*. *Am. Zool.* **36**, 666-677.
Daniel, T. L. (1984). Unsteady aspects of aquatic locomotion. *Integr. Comp. Biol.* **24**, 121-134.
Denny, M. W. (1990). Terrestrial versus aquatic biology: the medium and its message. *Integr. Comp. Biol.* **30**, 111-121.
Drucker, E. G. (1996). The use of gait transition speed in comparative studies of fish locomotion. *Am. Zool.* **36**, 555-566.
Drucker, E. G. and Lauder, G. V. (1999). Locomotor forces on a swimming fish: three-dimensional vortex wake dynamics quantified using digital particle image velocimetry. *J. Exp. Biol.* **202**, 2393-2412.
Drucker, E. G. and Lauder, G. V. (2000). A hydrodynamic analysis of fish swimming speed: wake structure and locomotor force in slow and fast labriform swimmers. *J. Exp. Biol.* **203**, 2379-2393.
Drucker, E. G. and Lauder, G. V. (2005). Locomotor function of the dorsal fin in rainbow trout: kinematic patterns and hydrodynamic forces. *J. Exp. Biol.* **208**, 4479-4494.
Eaton, T. H. (1945). Skeletal supports of the median fins of fishes. *J. Morphol.* **76**, 193-212.
Ferry, L. A. and Lauder, G. V. (1996). Heterocercal tail function in leopard sharks: a three-dimensional kinematic analysis of two models. *J. Exp. Biol.* **199**, 2253-2268.
Geerlink, P. J. and Videler, J. J. (1987). The relation between structure and bending properties of teleost fin rays. *Neth. J. Zool.* **37**, 59-80.
Gemballa, S. (2004). The musculoskeletal system of the caudal fin in the basal Actinopterygii: heterocercy, diphycercy, homocercy. *Zoomorphology* **123**, 15-30.
Gibb, A., Jayne, B. C. and Lauder, G. V. (1994). Kinematics of pectoral fin locomotion in the bluegill sunfish *Lepomis macrochirus*. *J. Exp. Biol.* **189**, 133-161.
Gibb, A. C., Dickson, K. A. and Lauder, G. V. (1999). Tail kinematics of the chub mackerel *Scomber japonicus*: testing the homocercal tail model of fish propulsion. *J. Exp. Biol.* **202**, 2433-2447.
Grove, A. J. and Newell, G. E. (1936). A mechanical investigation into the effectual action of the caudal fin in some aquatic chordates. *Ann. Mag. Nat. Hist.* **17**, 280-290.
Hatze, H. (1988). High-precision three-dimensional photogrammetric calibration and object space reconstruction using a modified DLT-approach. *J. Biomech.* **21**, 533-538.
Hedrick, T. L., Tobalske, B. W. and Biewener, A. A. (2002). Estimates of circulation and gait change based on a three-dimensional kinematic analysis of flight in cockatiels (*Nymphicus hollandicus*) and ringed turtle-doves (*Streptopelia risoria*). *J. Exp. Biol.* **205**, 1389-1409.
Hsieh, S. T. (2003). Three-dimensional hindlimb kinematics of water running in the plumed basilisk lizard (*Basiliscus plumifrons*). *J. Exp. Biol.* **206**, 4363-4377.
Jayne, B. C. and Lauder, G. V. (1993). Red and white muscle activity and kinematics of the escape response of the bluegill sunfish during swimming. *J. Comp. Physiol. A* **173**, 495-508.
Jayne, B. C. and Lauder, G. V. (1994). How swimming fish use slow and fast muscle fibers: implications for models of vertebrate muscle recruitment. *J. Comp. Physiol. A* **175**, 123-131.
Jayne, B. C. and Lauder, G. V. (1995a). Red muscle motor patterns during steady swimming in largemouth bass: effects of speed and correlations with axial kinematics. *J. Exp. Biol.* **198**, 1575-1587.
Jayne, B. C. and Lauder, G. V. (1995b). Speed effects on midline kinematics during steady undulatory swimming of largemouth bass, *Micropterus salmoides*. *J. Exp. Biol.* **198**, 585-602.
Jayne, B. C., Lozada, A. F. and Lauder, G. V. (1996). Function of the dorsal fin in bluegill sunfish: motor patterns during four distinct locomotor behaviors. *J. Morphol.* **228**, 307-326.
Lauder, G. V. (1982). Structure and function in the tail of the Pumpkinseed sunfish (*Lepomis gibbosus*). *J. Zool. Lond.* **197**, 483-495.
Lauder, G. V. (1989). Caudal fin locomotion in ray-finned fishes: historical and functional analyses. *Am. Zool.* **29**, 85-102.
Lauder, G. V. (2000). Function of the caudal fin during locomotion in fishes: kinematics, flow visualization, and evolutionary patterns. *Am. Zool.* **40**, 101-122.
Lauder, G. V. and Drucker, E. G. (2002). Forces, fishes, and fluids: hydrodynamic mechanisms of aquatic locomotion. *News Physiol. Sci.* **17**, 235-240.
Lauder, G. V. and Liem, K. F. (1983). The evolution and interrelationships of the Actinopterygian fishes. *Bull. Mus. Comp. Zool.* **150**, 95-197.
Lauder, G. V., Madden, P. G. A., Mittal, R., Dong, H. and Bozkurttas, M. (2006). Locomotion with flexible propulsors. I. Experimental analysis of pectoral fin swimming in sunfish. *Bioinspir. Biomim.* **1**, S25-S34.
Liao, J. and Lauder, G. V. (2000). Function of the heterocercal tail in white sturgeon: flow visualization during steady swimming and vertical maneuvering. *J. Exp. Biol.* **203**, 3585-3594.
Liem, K. F. (1970). Comparative functional anatomy of the Nandidae (Pisces: Teleostei). *Fieldiana Zool.* **56**, 7-164.
Liu, D. W. and Westerfield, M. (1988). Function of identified motoneurones and co-ordination of primary and secondary motor systems during zebrafish swimming. *J. Physiol.* **403**, 73-89.
McLean, D. L., Fan, J., Higashijima, S.-i., Hale, M. E. and Fetcho, J. R. (2007). A topographic map of recruitment in spinal cord. *Nature* **446**, 71-75.
Nag, A. C. (1967). Functional morphology of the caudal region of certain clupeiform and perciform fishes with reference to the taxonomy. *J. Morphol.* **123**, 529-558.
Nag, A. C. (1972). Ultrastructure and adenosine triphosphate activity of red and white muscle fibers of the caudal region of a fish, *Salmo gairdneri*. *J. Cell Biol.* **55**, 42-57.
Nag, A. C. and Nursall, J. R. (1972). Histogenesis of white and red muscle fibres of trunk muscles of a fish *Salmo gairdneri*. *Cytobios* **6**, 227-246.
Nauen, J. C. and Lauder, G. V. (2002). Quantification of the wake of rainbow trout (*Oncorhynchus mykiss*) using three-dimensional stereoscopic digital particle image velocimetry. *J. Exp. Biol.* **205**, 3271-3279.
Nursall, J. R. (1958). The caudal fin as a hydrofoil. *Evolution* **12**, 116-120.
Patruno, M., Radaelli, G., Mascarello, F. and Candia Carnevali, M. D. (1998). Muscle growth in response to changing demands of functions in the teleost *Sparus aurata* (L.) during development from hatching to juvenile. *Anat. Embryol.* **198**, 487-504.
Rome, L. C., Funke, R. P., Alexander, R. M. N., Lutz, G., Aldridge, H., Scott, F. and Freadman, M. (1988). Why animals have different muscle fiber types. *Nature* **335**, 824-827.
Rome, L. C., Swank, D. and Corda, D. (1993). How fish power swimming. *Science* **261**, 340-343.
Shadwick, R. E., Steffensen, J. F., Katz, S. L. and Knower, T. (1998). Muscle dynamics in fish during steady swimming. *Am. Zool.* **38**, 755-770.
Standen, E. M. and Lauder, G. V. (2005). Dorsal and anal fin function in bluegill sunfish *Lepomis macrochirus*: three-dimensional kinematics during propulsion and maneuvering. *J. Exp. Biol.* **208**, 2753-2763.
Syme, D. A. (2006). Functional properties of skeletal muscle. In *Fish Biomechanics*. Vol. 23 (ed. R. E. Shadwick and G. V. Lauder), pp. 173-232. San Diego: Elsevier Academic Press.
Tytell, E. D. (2006). Median fin function in bluegill sunfish *Lepomis macrochirus*: streamwise vortex structure during steady swimming. *J. Exp. Biol.* **209**, 1516-1534.
Tytell, E. D. and Lauder, G. V. (2002). The C-start escape response of *Polypterus senegalus*: bilateral muscle activity and variation during stage 1 and 2. *J. Exp. Biol.* **205**, 2591-2603.
Videler, J. J. (1975). On the interrelationships between morphology and movement in the tail of the cichlid fish *Tilapia nilotica* (L.). *Neth. J. Zool.* **25**, 143-194.
Webb, P. W. (1973). Kinematics of pectoral fin propulsion in *Cymatogaster aggregata*. *J. Exp. Biol.* **59**, 697-710.
Webb, P. W. and Smith, G. R. (1980). Function of the caudal fin in early fishes. *Copeia* **1980**, 559-562.
Winterbottom, R. (1974). A descriptive synonymy of the striated muscles of the Teleostei. *Proc. Acad. Nat. Sci. Philadelphia* **125**, 225-317.